RESEARCH ARTICLE
SPACE PHYSICS: MAGNETOSPHERIC PHYSICS

Earth and Planetary Physics
3: 204–211, 2019
doi: 10.26464/epp2019022

Heating of multi-species upflowing ion beams observed by Cluster on March 28, 2001

FangBo Yu[1], SuiYan Fu[1]*, WeiJie Sun[2], XuZhi Zhou[1], Lun Xie[1], Han Liu[1], Duo Zhao[1], ShaoJie Zhao[1], Li Li[1], JingWen Zhang[1], Tong Wu[1], and Ying Xiong[1]

[1]School of Earth and Space Sciences, Peking University, Beijing 100871, China;

[2]Department of Climate and Space Sciences and Engineering, University of Michigan, Ann Arbor, Michigan 48109, USA.

Abstract: Cluster satellites observed three successive outflowing ion beams on 28 March, 2001. It is generally accepted that these ion beams, composed of H^+, He^+, and O^+ ions, with three inverted-V structures in their energy spectra, are produced by acceleration through U-shaped potential structures. By eliminating the background ion population and employing Maxwelling fitting, we find that ions coming from the center of the potential structure have higher temperature than those from the flanks. Higher temperature of O^+ and He^+ compared to that of H^+ indicates that heavy ions are preferentially heated; we further infer that the heating efficiencies of O^+ and He^+ ions differ between the center and edges of the U-shaped potential structures. Estimation based on pitch angle observations shows that heating may also occur at an altitude above the upper boundary of the auroral acceleration region (AAR), where these beams are generally thought to be formed.

Keywords: oxygen; ion beams; inverted-V structures; U-shaped potential drop; preferentially heated heavy ions; heating above AAR

Citation: Yu, F. B., Fu, S. Y., Sun, W. J., Zhou, X. Z., Xie, L., Liu, H., Zhao, D., Zhao, S. J., Li, L., Zhang, J. W., Wu, T., and Xiong, Y. (2019). Heating of multi-species upflowing ion beams observed by Cluster on March 28, 2001. *Earth Planet. Phys.*, *3*(3), 204–211. http://doi.org/10.26464/epp2019022

1. Introduction

Ions from the ionosphere are widely observed in the magnetosphere. Their kinetic energy and temperature are much higher in the magnetosphere than in the ionosphere, indicating that they are significantly accelerated and heated during upflow processes (e.g., Moore et al., 1999).

The upflow regions include the polar caps, the auroral region, and the low/middle latitudes (e.g., Kronberg et al., 2014). The auroral region is generally regarded as the major source of ionospheric particles reaching the plasma sheet. It is believed that upflowing ion beams can be accelerated up to a few keV by quasi-static U-shaped electric potential structures between the ionosphere and the magnetosphere (e.g., Ergun et al., 1998; Marklund, 2009; Marklund et al., 2011), forming inverted-V structures in the ion energy spectra. The auroral acceleration region (AAR) is usually considered to have a lower boundary between ~2,000 to ~4,000 km (Shelley et al., 1976; Gorney et al., 1981; Morioka et al., 2009) and an upper boundary between 8,000 to 12,000 km (Paschmann et al., 2003; Cui YB et al., 2016). Over the past 50 years, a variety of mechanisms have been proposed to try to explain the existence and maintenance of the parallel electric fields in the AAR, including strong double layers (Block, 1972; Ergun et al., 2004), weak double layers (Temerin et al., 1982), anomalous resistivity (Hudson and Mozer, 1978), Alfvén waves (Song and Lysak, 2001), and magnetic mirror supported fields (Chiu and Schulz, 1978). However, the exact mechanism remains under debate.

The energies of outflowing H^+ and O^+ are closely related to solar activity. At least during solar minima, the heavier ions tend to reach higher energies (Möbius et al., 1998), which is not consistent with simple acceleration through a potential drop. An earlier study with DE (e.g. Collin et al., 1987) also showed that the ions in the beams were nominally at the same energy during solar maxima, but the energy of O^+ was higher during solar minima. It has been found that solar wind dynamic pressure may play an important role in ionospheric ion outflows. Echer et al. (2008) presented observations of O^+ ions from the ionosphere that were closely related to solar wind dynamic pressure pulses during the initial phase of a magnetic storm. Zong Q-G et al. (2008) have shown that ionospheric O^+ ions could dominate in the magnetotail plasma sheet during very intense magnetic storms. Korth et al. (2004) suggest that H^+ and O^+ ions have been accelerated to the same velocity possibly in the vicinity of a reconnection region. These observational facts are indirect evidence for preferential energization of ionospheric O^+ ions.

It is also believed that there is a heating process for ion beams moving from ionosphere to magnetosphere, during which the ion temperature increases significantly. This heating is usually considered to be a result of wave-particle resonance in the auroral region, where broadband low-frequency electromagnetic waves (Bonnell et al., 1996; Wahlund et al., 1998), lower hybrid waves

Correspondence to: S. Y. Fu, suiyanfu@pku.edu.cn
Received 02 MAR 2019; Accepted 01 APR 2019.
Accepted article online 29 APR 2019.

(Lynch et al., 1996), and electromagnetic ion cyclotron (EMIC) waves (Möbius et al., 1998) are usually observed. For broadband low-frequency electromagnetic waves, the heating efficiency is independent of ion mass (Knudsen et al., 1994; Norqvist et al., 1996). In contrast, the interaction between outflowing ions and EMIC waves shows higher heating efficiency for ions heavier than H^+ (Erlandson et al., 1994; Lund et al., 1998). For lower hybrid waves, the O^+ ions may be heated to higher energies than H^+ and He^+ (Lynch et al., 1999). However, lower hybrid waves may be responsible for ion heating mainly at altitudes below 2,000 km, giving ion energies of perhaps only a few eV (Kintner et al., 1992; Lynch et al., 1996).

Studies of ion heating mechanisms above the AAR are relatively rare. Cui YB et al. (2014) examined the properties of several ion beams with inverted-V structures above the AAR. They found that the parallel temperature of the ion beams tended to be higher at the energy peak of an inverted-V structure than on the flanks. However, the heating processes are still insufficiently understood, especially for different species. In this paper, we present observations of three successive ion beams with clear inverted-V structures in their energy spectrograms, and discuss the mechanisms responsible for differences in heating efficiency among H^+, He^+, and O^+.

2. Observation

Data from the Cluster mission (Escoubet et al., 2001) are employed in this study, including magnetic field data from the Fluxgate Magnetometer (FGM) (Balogh et al., 1997), ion composition measurements from the Composition and Distribution Function (CODIF) analyzer of the Cluster Ion Spectrometry (CIS) plasma experiment (Rème et al., 2001), and electromagnetic field power spectral densities from Spatio-Temporal Analysis of Field Fluctuations (STAFF) (Cornilleau-Wehrlin et al., 2003).

At ~23:00 UT on 28 March 2001, a series of inverted-V structures were detected by Cluster satellites SC1, SC3, and SC4 when they crossed the Northern Hemisphere high latitude plasma sheet boundary layer (PSBL). Figures 1a to 1c show the energy spectrograms of the H^+, He^+, and O^+ ions, respectively. At ~22:52 UT (marked by the black vertical dashed line in Figure 1), SC1 moved out from the central plasma sheet (CPS) and entered the PSBL, indicated by changes of ion populations from homogeneously thermalized distributions to non-homogeneous ones. Four minutes later, three successive inverted-V structures were observed at an altitude of ~21,000 km (marked by the red vertical dashed lines in panels (a)–(f)). These events are marked as 'I', 'II', and 'III' in Figure 1c. The peak energy of the inverted-V structures reached several keV, while the energy of the ions on both

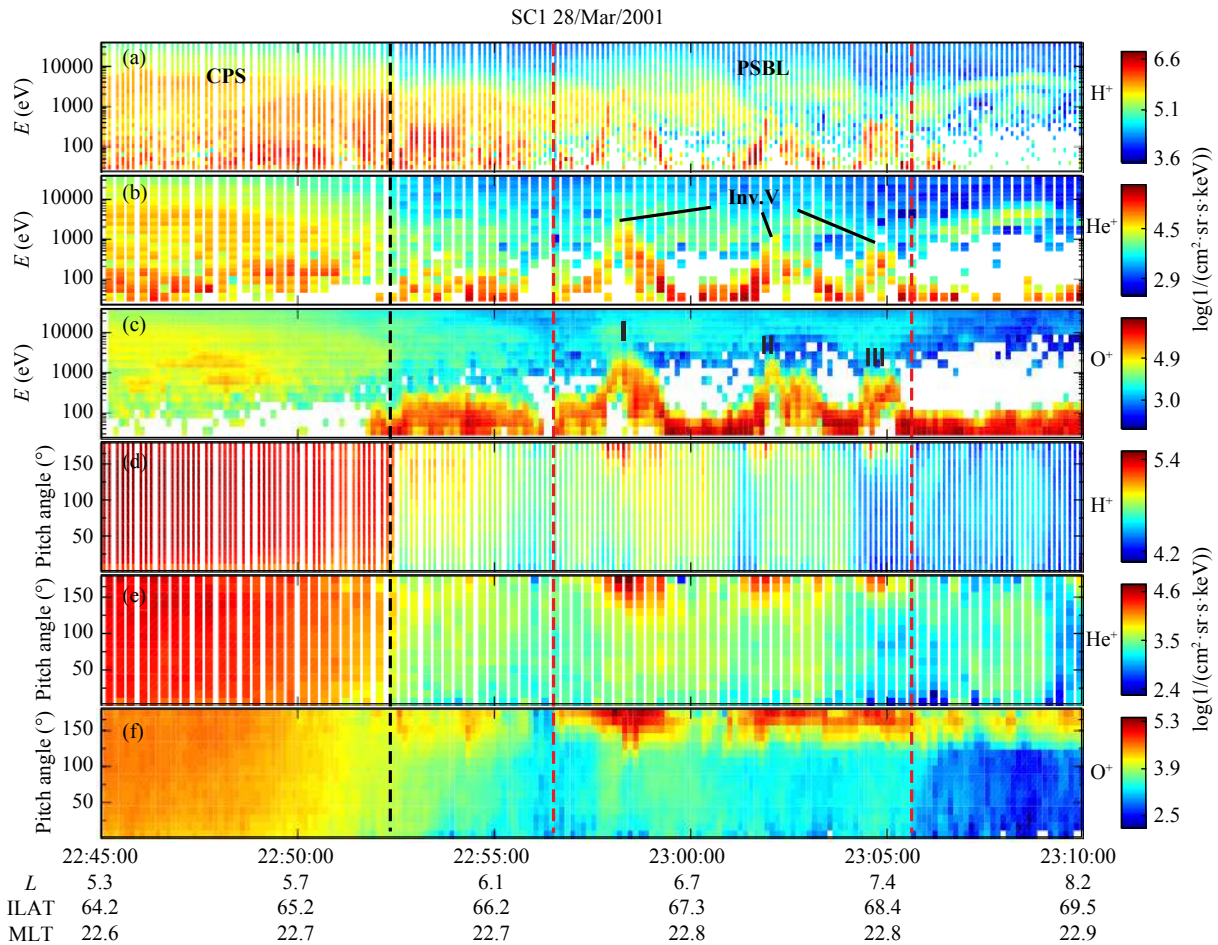

Figure 1. (a)–(c) Energy flux-time spectrograms for differential particle fluxes of H^+, He^+ and O^+ ions, as observed by Cluster SC1 between 22:45 and 23:10 UT on 28 March 2001. (d)–(f) H^+, He^+ and O^+ ion pitch angles in the energy range 21.5 eV to 38.4 keV over the same period.

flanks was only tens of eV.

Figures 1d to 1f present pitch angle distributions of the H^+, He^+, and O^+ ions, respectively, with an energy range from 21.5 eV to 38.4 keV. A particularly notable result is that particles were mainly distributed in the pitch angle range from 123.75° to 180°. Considering that the satellite was located in the Northern Hemisphere, we imply that these were outflowing ionospheric ions. At the same time, SC3 traveled through the PSBL in the Northern Hemisphere and observed three similar inverted-V structures at an altitude of ~20,000 km. About two minutes later, SC4 also detected three such structures at an altitude of ~20,000 km. The H^+, He^+, and O^+ observed by SC3 and SC4 were mainly distributed in the pitch angle range from ~150° to 180°. The range of pitch angles will be further discussed in Figure 4a.

Figures 2a to 2c presents the energy spectrograms of H^+, He^+, and O^+ with pitch angles ranging from 157.5° to 180°. The background population, which was assumed to have an isotropic distribution, was removed by subtracting an average differential flux of the ions with pitch angles ranging from 0° to 135°. The three inverted-V structures (labeled I, II and III) can be clearly observed in the energy spectrograms for all three ion species (compared to Figure 1a to 1c). There were intense electrostatic emissions at the energy peak of each inverted-V structure, and concentrated mainly below the lower hybrid frequency (~370 Hz, indicated by the horizontal black line in Figure 2d). SC3 and SC4 observed similar intense emissions (not shown). The magnetic power spectral densities in Figure 2e reveal that the magnetic fluctuations were enhanced at the center of inverted-V Structure I, with frequencies ranging from 7.76 to 40 Hz (the lowest frequency channel was between 7.76 and 9.78 Hz and the local cyclotron frequency for H^+ was ~8.65 Hz). These magnetic fluctuations were not observed by SC3 and SC4 in the same region. Positive gradients can be seen in the residual magnetic field (including dB_y and dB_z), indicating that there existed an upward current inside each inverted-V structure (Figure 2f).

Previous studies have attributed the inverted-V structures to ions

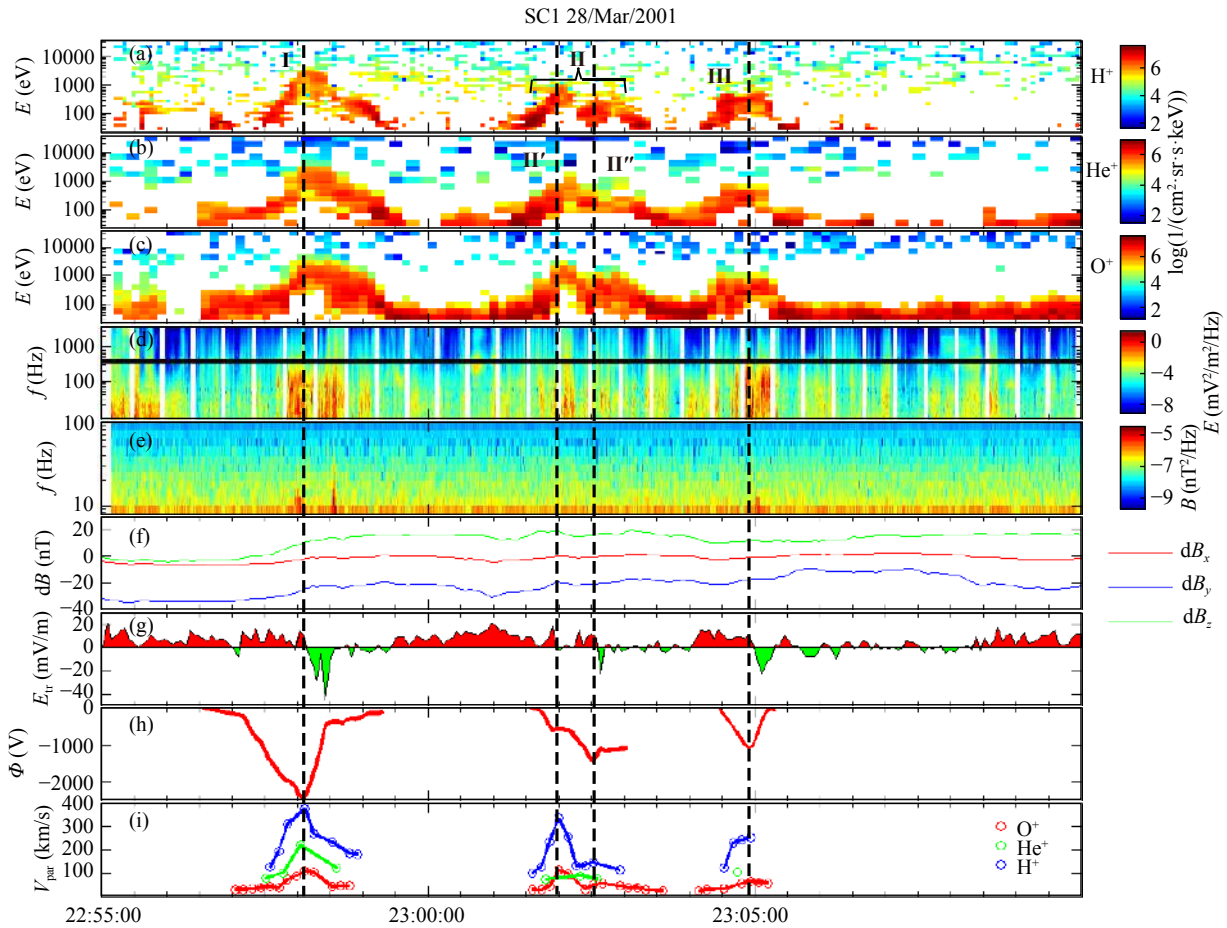

Figure 2. (a)–(c) Energy flux-time spectrograms for differential particle fluxes of H^+, He^+, and O^+ ions with pitch angles of between 157.5° and 180° observed by Cluster SC1 from 22:55 UT to 23:10 UT on 28 March 2001. The background population has been removed by subtracting the average differential particle flux of the ions with pitch angles of between 0° and 135°. (d) and (e) show the electric power spectral densities and magnetic power spectral densities in relation to frequency and time from STAFF. (f) shows the residual magnetic field component in the GSE, calculated by deducting the prediction of the T96 model from the magnetic field measured by SC1. (g) and (h) show the electric field component (E_{tr}) along the satellite orbit and the potential (Φ) obtained by integrating the electric field component along the SC1 orbit. (i) shows the streaming velocities (blue for H^+, green for He^+, and red for O^+) of the three outflowing beams.

accelerated by a quasi-static parallel electric field inside a U-potential drop (e.g., Marklund, 2009; Marklund et al., 2011; Sadeghi et al., 2011). In order to verify this scenario, we followed the method provided by Block and Fälthammar (1990) to obtain the electrical potential (Φ) by integrating $E_{\rm tr}$ from the beginning of the inverted-V structure to the end. The $E_{\rm tr}$ and potential are shown in Figures 2g and 2h. It can be seen in Figure 2g, that $E_{\rm tr}$ changed from positive (red) to negative (green) values at the peak of inverted-V Structures I and III, which is consistent with the model of the electric field strength of U-potential structures. Moreover, Figure 2h shows that the potential drops reached a maximum ~2.5 and ~1.1 kV inside inverted-V Structures I and III, respectively, which is almost the same value as the peak energy of the corresponding ion beams. This strongly supports the idea that the inverted-V structures of events I and III resulted from acceleration by a symmetrical U-shaped potential below the satellite. It is worth noting that the potential variation of Structure II might be asymmetric. The $E_{\rm tr}$ changed from positive (red) to negative (green) twice, at II′ and II″ (indicated by the second and third black vertical dashed lines from left to right), corresponding to the two energy peaks of inverted-V Structure II.

To study how the ion beams evolve along the magnetic field lines, we used a shifted Maxwellian distribution function to fit them and obtained the streaming velocity (v_b) and $T_{//}$ of the beams. The shifted Maxwellian distribution function can be written as follows:

$$f(v) = n_b\left(\frac{m}{2\,\pi\,k_B T_{//}}\right)^{3/2} \mathrm{e}^{\frac{-m(v-v_b)^2}{2k_B T_{//}}}, \qquad (1)$$

where n_b denotes the number density, $T_{//}$ is the parallel temperature, m is the ion mass, k_B is the Boltzmann constant, and v_b is the streaming velocity.

Figure 2i displays the fitting results for the streaming velocity (v_b) of the three outflowing beams. The streaming velocities of the H^+, He^+, and O^+ beams at the energy peak of inverted-V Structure I were ~400 ± 29.1 km/s, ~200 ± 23.7 km/s and ~100 ± 8.8 km/s, respectively, at a ratio of roughly 4:2:1. For Structure III, the ratio is also about 4:1 for velocities of the H^+ and O^+ beams at the energy peak. If all ion species experienced the same potential drop, they would gain the same amount of energy per charge. Therefore, the beam velocities of the different ion species should depend only on the charge-mass ratio, assuming that the thermal energy of the initial ionospheric particles is ignored. The comparable velocity ratios indicate that the H^+, He^+, and O^+ inside Structure I experienced the same potential drop, the same being largely the case for Structure III. However, for II-II′, the velocity ratio of the H^+ (~335 km/s) to O^+ (~111 km/s) was around 3:1.

Figure 3 presents 1D cuts through the distribution function in the parallel direcition with the background removed to emphasize the beams of inverted-V Structure I for SC1. Figure 3b shows that the $T_{//}$ of the H^+, He^+, and O^+ beams at the energy peak of Structure I, as observed by SC1, were 92.8 ± 10.9 eV, 115.0 ± 23.6 eV, and 146.5 ± 12.9 eV, respectively, which for all ion species were higher than those on the flanks. Note that the $T_{//}$ for the He^+ and O^+ ions were higher than those for the H^+. In addition, the O^+ beams had the highest parallel temperature among the three species at the energy peak of Structure I (see Figure 3b), while the He^+ ions showed the highest parallel temperature on both flanks (see Figures 3a and 3c). These observations indicate that the heating efficiency of O^+ and He^+ ions may differ between the center and the flanks of inverted-V Structure I.

Figure 4a shows the differential fluxes of O^+ at different pitch angles observed by SC1 (red), SC3 (green) and SC4 (blue) at the peaks of the inverted-V Structure I. It is clear that the differential particle flux detected by SC1 was significantly enhanced in the range from 123.75° to 180°. If only the mirror force is considered, the pitch angle will decrease when particles upflow to a higher altitude. Assuming that the ions were heated instantaneously at a fixed height, the pitch angles observed by SC1 would be related only to the original heating location where the pitch angles were supposed to be close to 90°. Therefore, by using the ion pitch angle distributions observed by SC1 and the magnetic field model, we can estimate the altitude of the heating region where ions were probably perpendicularly heated.

In Figure 4b, the blue lines indicate the maximum pitch angles of ions reaching SC1 if the heating occurs at a fixed height (the *X*-axis in this figure). Enhancement of the ions was concentrated in the pitch angle range from 123.75° to 180°. If the pitch angles of the ions were heated to the bin ranged from 123.75° to 135°, the calculated altitude where ions were heated should be above ~15,600 km, corresponding to 135° (marked as the third dashed green line from the left in Figure 4b). This means that, if the heating occurred exclusively below 15,600 km, the ions' pitch angle at this satellite altitude could not reach 135° and the enhancement of ions in this bin (123.75° to 135°) would not be observed by SC1. The observations from SC3 and SC4 indicate that the ion pitch angles closest to the perpendicular direction were 157.5° and 168.25°, respectively, meaning that the ions were heated at altitudes above ~8,600 and ~3,400 km. It is generally believed that the typical altitude of the upper boundary of the AAR does not exceed 12,000 km (Paschmann et al., 2003; Cui YB et al., 2016). Our results suggest that the ion beams present in inverted-V Structure I observed by SC1 may have been heated in a region above the upper boundary of the AAR.

3. Discussion and Summary

Three ion beams with inverted-V structures in the energy spectra were observed when Cluster SC1, SC3, and SC4 were travelling in the northern PSBL on March 28, 2001. The electric potential derived from the electric measurements and the ratios of parallel velocities of H^+, He^+, and O^+ (Structures I and III) suggest that these ions had been accelerated through a U-shaped potential drop before they were detected by the satellites.

It is well known that the acceleration of ions by electric potential may not change the ion temperature. However, the observations show that the $T_{//}$ of the H^+, He^+, and O^+ ions was ~100 eV (from SC1), which is significantly higher than the common upflowing ion temperature (several eVs) in the ionosphere (Lu et al., 1992). Therefore, there should be an additional heating process for these ions during the upflowing process. Heating mechanisms are mostly in the perpendicular direction and may change the subsequent perpendicular temperature. Observations have demon-

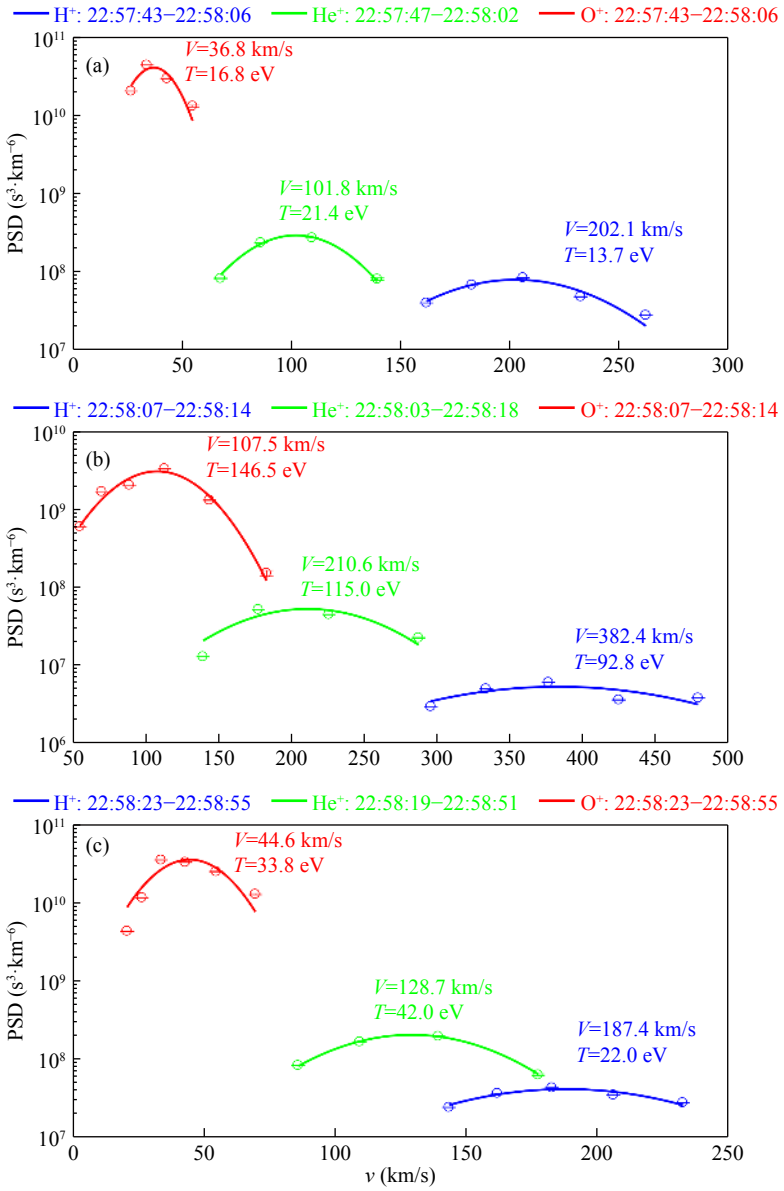

Figure 3. (a)–(c) 1D cuts of 3D velocity space distributions of H^+, He^+, and O^+ beams over three time periods observed by Cluster SC1, including the left flank of inverted-V Structure I during the time interval 22:57:43 to 22:58:06 UT, at Structure I's energy peak during the time interval 22:58:07 to 22:58:15 UT, and on its right flank during the time interval 22:58:23 to 22:58:55 UT. The background fluxes have been removed by adopting the same method used for Figure 2(a–c), with the best Maxwellian fit being shown on top of the distribution.

strated that the heating process in the auroral region commonly involves electromagnetic waves, such as those in the broadband low-frequency range (Bonnell et al., 1996; Wahlund et al., 1998), lower hybrid waves (Lynch et al., 1996) and EMIC waves (Möbius et al., 1998; Lund et al., 1998). EMIC waves with frequencies below the gyro-frequency of heavy ions will eventually become gyro-resonant with the ions (Temerin and Roth, 1986). Previous work indicates that such energization by EMIC waves often occurs below 4,200 km (Erlandson et al., 1994; Lund et al., 1998). Taking account of the structure of the Earth's magnetic field, it is reasonable to assume that part of the perpendicular energy in a lower altitude in the auroral region could be adiabatically transferred into parallel energy at a higher altitude. Referring to the calculation results shown in Figure 4b, if the heating occurred at ~4,000 km in the perpendicular direction, the pitch angles would be changed to not less than 157.5° by the mirror force when the ions reached the location of SC1. It also means the change of ions distributions by EMIC waves at ~4,000 km will eventually influence the $T_{//}$ for ions in this event. Previous studies show that the heating of heavy ions by EMIC waves is more efficient than of H^+ ions (Möbius et al., 1998). Our observations show that the $T_{//}$ of He^+ and O^+ ions were higher than those of H^+, which is consistent with the prediction based on the earlier scenario. Previous research also demonstrated that auroral EMIC waves are observed at frequencies between f_{He^+} and f_{H^+} with their heating of He^+ being the most pronounced (Lund et al., 1998), and at frequencies below f_{O^+} giving a preferential acceleration to O^+ (Erlandson et al., 1994). We found that the $T_{//}$ of the O^+ ions was the highest among the three spe-

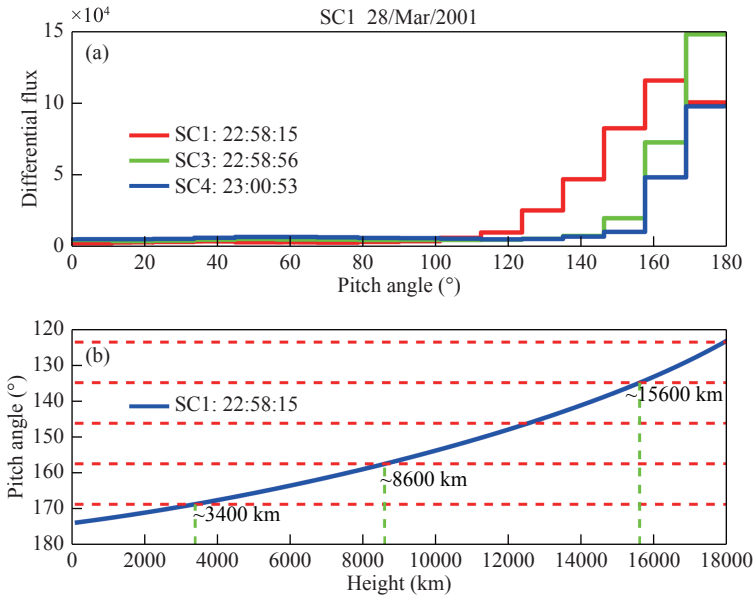

Figure 4. (a) The differential particle flux of O^+ ions at the energy peak of the inverted-V Structure I observed by the satellites SC1 (red), SC3 (green), and SC4 (blue). (b) The relationship between the pitch angles of the O^+ ions in the inverted-V Structure I observed by SC1 at 22:58:15 UT and their corresponding source altitudes. The dashed red lines denote each pitch angle channel acquired by the CODIF instrument, i.e. 168.75°, 157.5°, 145.25°, 135°, and 123.75°, from bottom to top. The dashed green lines denote the heating altitudes corresponding to the pitch angle channel closest to 90° observed by SC1, SC3, and SC4 (from right to left).

cies at the energy peak of inverted-V Structure I, while the $T_{//}$ of the He^+ beams was the highest on the flanks. The fact that this heating mechanism shows mass dependence at the center and edges of the U-shaped potential structures suggests that EMIC waves participating in the wave-particle interaction may have different frequencies at different locations relative to the potential. In addition, ions of different masses at the same energy will travel at different velocities, possibly leading to development of a two-stream instability that will transfer energy from lighter to heavier ions (Möbius et al., 1998). Particle simulations for mixed H^+, He^+, and O^+ beams by Winglee et al. (1989) have confirmed that this scenario is viable.

The other prominent point needing to be mentioned is that SC1 observed a wide pitch angle coverage (123.75° to 180°) at the energy peak of Structure I, which can not be explained solely by heating within the AAR; if the heating occurred below 15,600 km, the ions observed at this satellite altitude should be mostly in the parallel direction and their pitch angle could not reach 135°. The observed data suggest that after being energized by the parallel electric field and EMIC waves inside the AAR, extra heating occurred above the upper boundary of the AAR. The magnetic field data from STAFF show enhanced fluctuations between ~8 Hz (the lower limit of the instrument) and 40 Hz around the energy peak. This frequency range covers the local cyclotron frequency of H^+ (~8.65 Hz), which means that broadband low-frequency electromagnetic waves may be playing a role in extra heating above the AAR through wave-particle resonance (Chang et al., 1986; Lund et al., 1999). However, the weak intensity limits our analysis of these waves; thus, other possibilities cannot be ruled out at this time. It is worth noting that similar fluctuations in the magnetic field were not captured by SC4. As SC4 observed a lower and longer duration of the peak energy value than SC1, it is likely that SC4 went through the edge of the U-shaped potential structures, while the trajectory of SC1 may have cut through the center. One implication is that the electromagnetic waves involved in this phenomenon may be highly localized above the center of the U-shaped structure.

Our main conclusions are summarized as follows:

(1) The electric potentials derived from the electric measurements and parallel velocity ratios for H^+, He^+, and O^+ (Structures I and III) suggest that the ions in the inverted-V structures were accelerated by symmetric U-shaped potentials. In addition, ions coming from the center of the potential structure have higher temperature than those from the flanks.

(2) O^+ and He^+ ions are preferentially heated. We found that the $T_{//}$ of the O^+ ions was the highest among the three species at the energy peak of the inverted-V Structure I, while the $T_{//}$ of the He^+ ions was the highest on the flanks. We infer that the heating efficiencies of O^+ and He^+ ions vary between the center and edges of the U-shaped potential structures.

(3) The range of the ion pitch angles for the energy peak of the inverted-V Structure I observed by SC1 was from 123.75° to 180°. Estimation based on the pitch angle observations shows that the ions in Structure I were heated above ~ 15,600 km, which is above the upper boundary of the AAR.

Acknowledgments

The data used in this study were obtained from the Cluster Science Archive (CSA): http://cosmos.esa.int/. We are grateful to the Cluster FGM, CIS, STAFF, and EFW teams and the CSA for providing these high-quality data. This work has been supported by the National Natural Science Foundation of China (grants 41474139,

41731068, and 41704163).

References

Balogh, A., Dunlop, M. W., Cowley, S. W. H., Southwood, D. J., Thomlinson, J. G., Glassmeier, K. H., Musmann, G., Lühr, H., Buchert, S., … Kivelson, M. G. (1997). The cluster magnetic field investigation. *Space Sci. Rev.*, *79*(1-2), 65–91. https://doi.org/10.1023/A:1004970907748

Block, L. P. (1972). Potential double layers in the ionosphere. *Cosmic Electrodyn.*, *3*, 349.

Block, L. P., and Fälthammar, C. G. (1990). The role of magnetic-field-aligned electric fields in auroral acceleration. *J. Geophys. Res. Space Phys.*, *95*(A5), 5877–5888. https://doi.org/10.1029/JA095iA05p05877

Bonnell, J., Kintner, P., Wahlund, J. E., Lynch, K., and Arnoldy, R. (1996). Interferometric determination of broadband ELF wave phase velocity within a region of transverse auroral ion acceleration. *Geophys. Res. Lett.*, *23*(23), 3297–3300. https://doi.org/10.1029/96GL03238

Chang, T., Crew, G. B., Hershkowitz, N., Jasperse, J. R., Retterer, J. M., and Winningham, J. D. (1986). Transverse acceleration of oxygen ions by electromagnetic ion cyclotron resonance with broad band left-hand polarized waves. *Geophys. Res. Lett.*, *13*(7), 636–639. https://doi.org/10.1029/GL013i007p00636

Chiu, Y. T., and Schulz, M. (1978). Self-consistent particle and parallel electrostatic field distributions in the magnetospheric-ionospheric auroral region. *J. Geophys. Res. Space Phys.*, *83*(A2), 629–642. https://doi.org/10.1029/JA083iA02p00629

Collin, H. L., Peterson, W. K., and Shelley, E. G. (1987). Solar cycle variation of some mass dependent characteristics of upflowing beams of terrestrial ions. *J. Geophys. Res. Space Phys.*, *92*(A5), 4757–4762. https://doi.org/10.1029/JA092iA05p04757

Cornilleau-Wehrlin, N., Chanteur, G., Perraut, S., Rezeau, L., Robert, P., Roux, A., de Villedary, C., Canu, P., Maksimovic, M., … Le Contel, O. (2003). First results obtained by the Cluster STAFF experiment. *Ann. Geophys.*, *21*(2), 437–456. https://doi.org/10.5194/angeo-21-437-2003

Cui, Y. B., Fu, S. Y., and Parks, G. K. (2014). Heating of ionospheric ion beams in inverted-V structures. *Geophys. Res. Lett.*, *41*(11), 3752–3758. https://doi.org/10.1002/2014GL060524

Cui, Y. B., Fu, S. Y., Zong, Q. G., Xie, L., Sun, W. J., Zhao, D., Wu, T., and Parks, G. (2016). Altitude of the upper boundary of AAR based on observations of ion beams in inverted-V structures: A case study. *Sci. China Earth Sci.*, *59*(7), 1489–1497. https://doi.org/10.1007/s11430-016-0019-3

Echer, E., Korth, A., Zong, Q. G., Fraünz, M., Gonzalez, W. D., Guarnieri, F. L., Fu, S. Y., and Reme, H. (2008). Cluster observations of O^+ escape in the magnetotail due to shock compression effects during the initial phase of the magnetic storm on 17 August 2001. *J. Geophys. Res. Space Phys.*, *113*(A5), A05209. https://doi.org/10.1029/2007JA012624

Ergun, R. E., Carlson, C. W., McFadden, J. P., Mozer, F. S., Delory, G. T., Peria, W., Chaston, C. C., Temerin, M., Roth, I., … Kistler, L. (1998). FAST satellite observations of large-amplitude solitary structures. *Geophys. Res. Lett.*, *25*(12), 2041–2044. https://doi.org/10.1029/98GL00636

Ergun, R. E., Andersson, L., Main, D., Su, Y. J., Newman, D. L., Goldman, M. V., Carlson, C. W., Hull, A. J., McFadden, J. P., and Mozer, F. S. (2004). Auroral particle acceleration by strong double layers: The upward current region. *J. Geophys. Res. Space Phys.*, *109*(A12), A12220. https://doi.org/10.1029/2004JA010545

Erlandson, R. E., Zanetti, L. J., Acuña, M. H., Eriksson, A. I., Eliasson, L., Boehm, M. H., and Blomberg, L. G. (1994). Freja observations of electromagnetic ion cyclotron ELF waves and transverse oxygen ion acceleration on auroral field lines. *Geophys. Res. Lett.*, *21*(17), 1855–1858. https://doi.org/10.1029/94GL01363

Escoubet, C. P., Fehringer, M., and Goldstein, M. (2001). Introduction: The Cluster mission. *Ann. Geophys.*, *19*(10-12), 1197–1200. https://doi.org/10.5194/angeo-19-1197-2001

Gorney, D. J., Clarke, A., Croley, D., Fennell, J., Luhmann, J., and Mizera, P. (1981). The distribution of ion beams and conics below 8000 km. *J. Geophys. Res. Space Phys.*, *86*(A1), 83–89. https://doi.org/10.1029/JA086iA01p00083

Hudson, M. K., and Mozer, F. S. (1978). Electrostatic shocks, double layers, and anomalous resistivity in the magnetosphere. *Geophys. Res. Lett.*, *5*, 131. https://doi.org/10.1029/GL005i002p00131

Kintner, P. M., Vago, J., Chesney, S., Arnoldy, R. L., Lynch, K. A., Pollock, C. J., and Moore, T. E. (1992). Localized lower hybrid acceleration of ionospheric plasma. *Phys. Rev. Lett.*, *68*(16), 2448–2451. https://doi.org/10.1103/PhysRevLett.68.2448

Knudsen, D. J., Whalen, B. A., Abe, T., and Yau, A. (1994). Temporal evolution and spatial dispersion of ion conics: evidence for a polar cusp heating wall. In J. L. Burch, et al. (Eds.), *Solar System Plasmas in Space and Time* (pp. 163-169). Washington DC: American Geophysical Union. https://doi.org/10.1029/GM084p0163

Korth, A., Fränz, M., Zong, Q. G., Fritz, T. A., Sauvaud, J. A., Rème, H., Dandouras, I., Friedel, R., Mouikis, C. G., … Daly, P. W. (2004). Ion injections at auroral latitude during the March 31, 2001 magnetic storm observed by Cluster. *Geophys. Res. Lett.*, *31*(20), L20806. https://doi.org/10.1029/2004GL020356

Kronberg, E. A., Ashour-Abdalla, M., Dandouras, I., Delcourt, D. C., Grigorenko, E. E., Kistler, L. M., Kuzichev, I. V., Liao, J., Maggiolo, R., … Zelenyi, L. M. (2014). Circulation of heavy ions and their dynamical effects in the magnetosphere: Recent observations and models. *Space Sci. Rev.*, *184*(1-4), 173–235. https://doi.org/10.1007/s11214-014-0104-0

Lu, G., Reiff, P. H., Moore, T. E., and Heelis, R. A. (1992). Upflowing ionospheric ions in the auroral region. *Journal of Geophysical Research*: *Space Physics*, *97*(A11), 16855–16863. https://doi.org/10.1029/92JA01435

Lund, E. J., Möbius, E., Tang, L., Kistler, L. M., Popecki, M. A., Klumpar, D. M., Peterson, W. K., Shelley, E. G., Klecker, B., … Pfaff R. F. (1998). FAST observations of preferentially accelerated He^+ in association with auroral electromagnetic ion cyclotron waves. *Geophys. Res. Lett.*, *25*(12), 2049–2052. https://doi.org/10.1029/98GL00304

Lund, E. J., Möbius, E., Klumpar, D. M., Kistler, L. M., Popecki, M. A., Klecker, B., Ergun, R. E., McFadden, J. P., Carlson, C. W., and Strangeway, R. J. (1999). Direct comparison of transverse ion acceleration mechanisms in the auroral region at solar minimum. *J. Geophys. Res. Space Phys.*, *104*(A10), 22801–22805. https://doi.org/10.1029/1999JA900265

Lynch, K. A., Arnoldy, R. L., Kintner, P. M., and Bonnell, J. (1996). The AMICIST auroral sounding rocket: A comparison of transverse ion acceleration mechanisms. *Geophys. Res. Lett.*, *23*(23), 3293–3296. https://doi.org/10.1029/96GL02688

Lynch, K. A., Arnoldy, R. L., Kintner, P. M., Schuck, P., Bonnell, J. W., and Coffey, V. (1999). Auroral ion acceleration from lower hybrid solitary structures: A summary of sounding rocket observations. *J. Geophys. Res. Space Phys.*, *104*(A12), 28515–28534. https://doi.org/10.1029/1999JA900289

Marklund, G. T. (2009). On the ionospheric coupling of auroral electric fields. *Nonlin. Processes Geophys.*, *16*(2), 365–372. https://doi.org/10.5194/npg-16-365-2009

Marklund, G. T., Sadeghi, S., Karlsson, T., Lindqvist, P. A., Nilsson, H., Forsyth, C., Fazakerley, A., Lucek, E. A., and Pickett, J. (2011). Altitude distribution of the auroral acceleration potential determined from cluster satellite data at different heights. *Phys. Rev. Lett.*, *106*(5), 055002. https://doi.org/10.1103/PhysRevLett.106.055002

Möbius, E., Tang, L., Kistler, L. M., Popecki, M., Lund, E. J., Klumpar, D., Peterson, W., Shelley, E. G., Klecker, B., … Pfaff, R. (1998). Species dependent energies in upward directed ion beams over auroral arcs as observed with FAST TEAMS. *Geophys. Res. Lett.*, *25*(12), 2029–2032. https://doi.org/10.1029/98GL00381

Moore, T. E., Lundin, R., Alcayde, D., André, M., Ganguli, S. B., Temerin, M., and Yau, A. (1999). Source processes in the high-latitude ionosphere. *Space Sci. Rev.*, *88*(1-2), 7–84. https://doi.org/10.1023/A:1005299616446

Morioka, A., Miyoshi, Y., Tsuchiya, F., Misawa, H., Yumoto, K., Parks, G. K., Anderson, R. R., Menietti, J. D., and Honary, F. (2009). Vertical evolution of auroral acceleration at substorm onset. *Ann. Geophys.*, *27*(2), 525–535. https://doi.org/10.5194/angeo-27-525-2009

Norqvist, P., André, M., Eliasson, L., Eriksson, A. I., Blomberg, L., Lühr, H., and Clemmons, J. H. (1996). Ion cyclotron heating in the dayside magnetosphere. *J. Geophys. Res. Space Phys.*, *101*(A6), 13179–13193.

https://doi.org/10.1029/95JA03596

Paschmann, G., Haaland, S., and Treumann, R. (2003). *Auroral Plasma Physics*. Dordrecht: Springer. https://doi.org/10.1007/978-94-007-1086-3

Rème, H., Aoustin, C., Bosqued, J. M., Dandouras, I., Lavraud, B., Sauvaud, J. A., Barthe, A., Bouyssou, J., Camus, T., … Scudder, J. (2001). First multispacecraft ion measurements in and near the Earth's magnetosphere with the identical Cluster ion spectrometry (CIS) experiment. *Ann. Geophys.*, *19*(10-12), 1303–1354. https://doi.org/10.5194/angeo-19-1303-2001

Sadeghi, S., Marklund, G. T., Karlsson, T., Lindqvist, P. A., Nilsson, H., Marghitu, O.,... Lucek, E. A. (2011). Spatiotemporal features of the auroral acceleration region as observed by Cluster. *J Geophys Res*: *Space Physics*, *116*(A1). https://doi.org/10.1029/2011JA016505

Shelley, E. G., Sharp, R. D., and Johnson, R. G. (1976). Satellite observations of an ionospheric acceleration mechanism. *Geophys. Res. Lett.*, *3*(11), 654–656. https://doi.org/10.1029/GL003i011p00654

Song, Y., and Lysak, R. L. (2001). Towards a new paradigm: from a quasi-steady description to a dynamical description of the magnetosphere. *Space Sci. Rev.*, *95*(1-2), 273–292. https://doi.org/10.1023/A:1005288420253

Temerin, M., Cerny, K., Lotko, W., and Mozer, F. S. (1982). Observations of double layers and solitary waves in the auroral plasma. *Phys. Rev. Lett.*, *48*(17), 1175–1179. https://doi.org/10.1103/PhysRevLett.48.1175

Temerin, M., and Roth, I. (1986). Ion heating by waves with frequencies below the ion gyrofrequency. *Geophys. Res. Lett.*, *13*(11), 1109–1112. https://doi.org/10.1029/GL013i011p01109

Wahlund, J. E., Eriksson, A. I., Holback, B., Boehm, M. H., Bonnell, J., Kintner, P. M., Seyler, C. E., Clemmons, J. H., Eliasson, L., … Zanetti, L. J. (1998). Broadband ELF plasma emission during auroral energization: 1.Slow ion acoustic waves. *J. Geophys. Res. Space Phys.*, *103*(A3), 4343–4375. https://doi.org/10.1029/97JA02008

Winglee, R. M., Dusenbery, P. B., Collin, H. L., Lin, C. S., and Persoon, A. M. (1989). Simulations and observations of heating of auroral ion beams. *J. Geophys. Res. Space Phys.*, *94*(A7), 8943–8965. https://doi.org/10.1029/JA094iA07p08943

Zong, Q. G., Zhang, H., Fu, S. Y., Wang, Y. F., Pu, Z. Y., Korth, A., Daly, P. W., and Fritz, T. A. (2008). Ionospheric oxygen ions dominant bursty bulk flows: Cluster and Double Star observations. *J. Geophys. Res. Space Phys.*, *113*(A7), A07S23. https://doi.org/10.1029/2007JA012764